JOURNAL OF MATERIALS SCIENCE 33 (1998) 4131–4139

Stress relaxation of starch/synthetic polymer blends

M. BHATTACHARYA
Department of Biosystems and Agricultural Engineering, Univeristy of Minnesota, St. Paul, MN 55108, USA
E-mail: bhaH002@maroon.tc.umn.edu

Stress relaxation behaviour of injection-moulded starch/synthetic polymer blends were studied. In one experiment, the starch content was kept constant at 70% while the amylose to amylopectin ratio was varied. The synthetic polymers in the blend included high-density (HPDE) and low-density polyethylene (LPDE), and ethylene vinyl acetate (EVA). In the second experiment, the starch content in the blend was varied. A small amount of maleic anhydride-functionalized synthetic polymer (5% by weight) was added to compatibilize reactively the starch and the synthetic polymer. Starch/HDPE and starch/LPDE blends had a ductile behaviour, while starch/EVA blends displayed rubbery characteristics. Blends containing EVA relaxed the fastest while those containing LPDE took the longest time. A double logarithmic plot of stress versus time at constant strain was linear and the slopes of the plots were insensitive to starch type but were affected by the starch content. Residual internal stress which developed during moulding was also estimated from the stress relaxation measurement. The stress–relaxation data fitted several empirical stress–time non-linear models well.

1. Introduction

In recent years there has been significant interest in developing materials from blends of natural and synthetic polymers. These blends can be processed into useful disposable end products that could alleviate the disposal problem by degrading in selective environments. The mechanical properties of polymer blends depend greatly on the adhesion of phases. Poor interfacial adhesion leads to lower ultimate properties, while strong interfacial adhesion leads to good mechanical properties and reduced molecular mobility, due to packing of macromolecules adjacent to the interface. In addition, when processed using various techniques, these materials and products develop internal stresses. For example, injection-moulded specimens display a inhomogeneous internal stress field that is compressive at the surface, while tensile stresses dominate the interior [1]. The viscoelastic nature of the melt results in the development of shear and normal stresses due to deformation during the filling state. These stresses are frozen-in because of the difference in the solidification rate between the surface parts and the interior of the object, and result in incomplete relaxation during the cooling stage. Molecular orientation is induced in the sample if the cooling rate is large enough to prevent random molecular conformation following flow.

The work reported here deals with the viscoelastic response of injection-moulded starch/synthetic polymer blends by means of stress relaxation experiments. These experiments are useful in predicting the long-term mechanical behaviour of materials from short-time experiments. Data have been obtained using starches of different compositions (amylopectin to amylose ratio), each blended with three different types of polyolefins (high-density and low-density polyethylene, and ethylene vinyl acetate) as well as varying the amount of starch in each blend. Starch is composed of repeating 1,4-α-D-glucopyranosyl units, and is a mixture of amylose (linear structure) and amylopectin (branched structure) units. The molecular weights of amylose and amylopectin in the starches are normally of the order of several hundred thousands and several millions, respectively. Commonly used starches have an amylose content of 25%.

There are two fundamental types of transient experiments that can be used to assess the viscoelastic properties with time. These are stress relaxation and creep. In the stress relaxation mode, the time decay of stress at a constant strain can be determined; in creep the decrease of strain with constant stress is investigated. In addition, as shown by Kubat and co-workers [2–4], the stress relaxation procedure can be adapted to obtain the internal stresses in the polymer using a slight variation of the method proposed by Li [5]. For both metals and polymers, the internal stress level affects the kinetics of creep and stress relation [6, 7] and this is exploited to determine the internal stress of the polymers.

2. Experimental procedure

2.1. Materials

Industrial corn starch (SMP 1100) containing approximately 25% amylose and 75% amylopectin was obtained from Cargill, Incorporated. Waxy (100% amylopectin) and high amylose corn starches (50% and 70% amylose) were obtained from National Starch Incorporated. Ethylene vinyl acetate (EVA) (ELVAX 240, melt flow index ≈ 43), ethylene vinyl acetate maleic anhydride (EVAMA) (MC-190D, melt flow index ≈ 20), low-density polyethylene maleic anhydride (EMA) (MB-110D, melt flow index ≈ 40) and high-density polyethylene maleic anhydride (HDPEMA, MB 265D, melt flow index ≈ 7) were obtained from DuPont (Kingston, Canada). These maleated polymers are sold under the trade name of FUSABOND. Low-density polyethylene (LPDE, melt flow index ≈ 8) and high-density polyethylene (HDPE, melt-flow index ≈ 9) were obtained from Dow Chemical Co. (Midlands, MI). The vinyl acetate content in the EVA was 28 mol %. The maleic anhydride content of EVAMA, HDPEMA, and EMA was approximately 0.8 mol %. The starch content was kept constant at 70% in all blends.

2.2. Sample preparation

Starch and synthetic polymer blends were melt-compounded in a co-rotating extruder using conditions described elsewhere [8]. Each blend composition contained 70% starch, 5% functionalized polymer (HDPEMA, EMA, or EVAMA), and 25% non-functionalized polymer (HPDE, LLDPE, or EVA). In a second study, to delineate the effect of starch, blends containing 15%, 30%, 50% and 60% normal starch were blended with the synthetic polymer and compatibilizer which were kept constant at 5% level for all blends. Injection-moulded samples were prepared to form ASTM D-638-68 Type I dog-bone specimens, approximately 3 mm thick, using a single-gated mould, thus avoiding the formation of any weldlines. The processing conditions for the various blends during extrusion and injection moulding are summarized in Tables I and II, respectively. All samples were tested approximately 48 h after injection moulding was accomplished.

2.3. Stress relaxation measurements

The tensile testing of the samples was done using an MTS universal tester. Stress is the measured force per unit cross-sectional area of the original sample. The samples were marked representing an initial jaw separation of approximately 4.6 ± 0.2 cm. The length was measured using calipers which permitted estimates to be made to a tenth of a millimetre. The strain rate was $1.2 \times 10^{-3}\,s^{-1}$. The gauge length at any time was calculated from the time elapsed from the start of the test and the crosshead speed. Per cent elongation is the ratio of the change in the gauge length at any time to the original gauge length of the sample. Elongation results are compared on the basis of time to the stoppage of the machine. Strain, ε, was determined as the ratio of the change in length to the original length. The experimental results of load versus elongation were converted into true stress versus strain, where the true stress is equal to $(1 + \varepsilon)$ times the engineering stress. For starch/HDPE and starch/LDPE, this correction has a negligible effect, because the elongation is small. Stress relaxation experiments were performed on the blends at room temperature by deforming the sample, maintaining a constant deformation, and measuring the stress as a function of time. By varying the initial stress, σ_0, a number of curves can be produced. Samples were stressed to approximately 20%, 35%, 50%, 65% and 80% maximum stress to yield. The decay in stress was monitored with time for approximately 2500 s. For each test a fresh specimen was used. To obtain the internal stress, the procedure given by Li [5] was used. The recorded relaxation data were transformed into stress–log (time) curves, and the slope of the rectilinear portion of the curves

$$F = \left(-\frac{d\sigma}{d \log t} \right) \quad (1)$$

was plotted against the corresponding stress, σ, during the relaxation experiment. The intercept of the resulting curve with the stress axis is the internal stress level, σ_i. Alternately, the maximum slope of the stress–log(time) curves is plotted with the initial stress σ_0, and the intercept of the resulting curve with the stress axis is the internal stress level, σ_i. This is the Kubat–Righdahl (KR) procedure [2]. In Li's method, a single curve is needed to obtain the initial stress while a series of tests conducted at different σ_0 is needed to obtain the internal stress level σ_i.

TABLE I Processing conditions of starch blends during compounding

Parameters	Blend type		
	EVA	LDPE	HDPE
Feed section temperature (°C)	80	80	115
First zone temperature (°C)	140	150	150
Second zone temperature (°C)	150	150	150
Die temperature (°C)	100	110	135
Screw speed (r.p.m.)	60	60	60

TABLE II Injection-moulding conditions

Parameters	Blend type		
	EVA	LDPE	HDPE
Melt temperature (°C)	170	155	155
Mould temperature (°C)	20	40	45
Back pressure (MPa)	4	0.5	0.5
Injection pressure (MPa)	12	8	8
Screw speed (RPM)	100	100	100

3. Results

The stress–strain behaviour of blends of starch and the three different polyolefins is shown in Fig. 1.

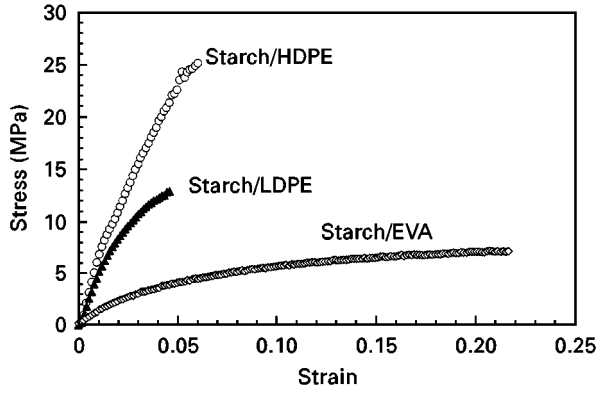

Figure 1 Stress–strain plot for starch/HDPE, starch/LDPE, and starch/EVA blends containing 70% starch.

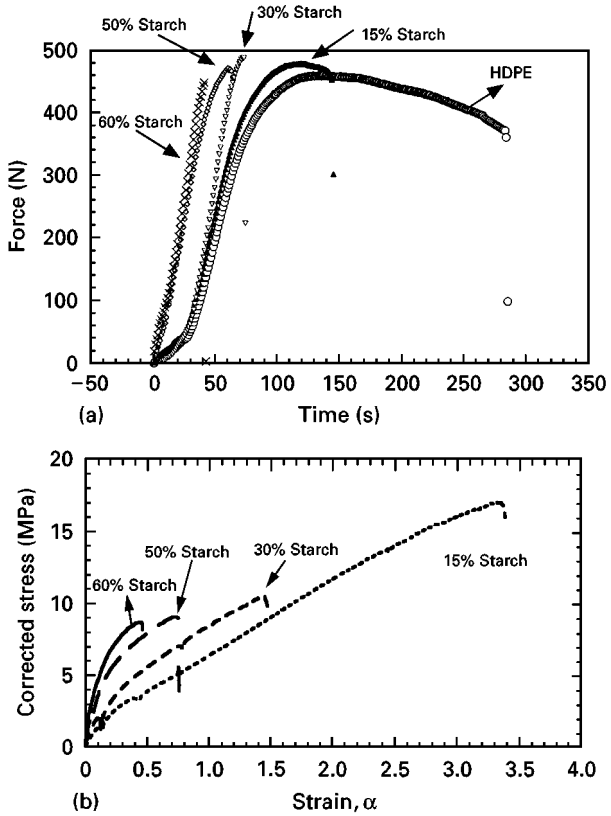

Figure 2 (a) Force–time plot of starch/HDPE blends containing different starch contents. (b) Stress–strain plot of starch/EVA blends containing different starch content. Note the stress has been corrected for varying cross-sectional area due to deformation.

Starch/HDPE and starch/LDPE blends exhibit stress–strain curves similar to that of ductile polymers while with starch/EVA blends the material is more rubbery. The elastic modulus of starch/HDPE and starch/LDPE blends range between 450 and 550 MPa for the various types of starch at the 70% level, while for starch/EVA blends the elastic modulus ranges from 80–110 MPa for the 70% starch level. The stress–strain behaviour as a function of starch content for starch/HDPE blends and starch/EVA blends is shown in Fig. 2a and b, respectively. As the starch content is increased, the modulus of the blends increases as the per cent elongation decreases.

3.1. Stress relaxation

Because most polymers exhibit a slow relaxation mechanism, it is difficult to continue experiments until a "true" elastic equilibrium state is achieved. In reality, very few of the blends reach an equilibrium value when stress versus time plots are examined. A stress versus time plot conducted over 64 h, shown in Fig. 3, shows that the material still has not achieved true equilibrium. Representative stress relaxation plots for the blends of various types of starch and synthetic polymers containing 70% starch of different amylose contents, are shown in Fig. 4a–c. It is observed that for every blend composition, the stress drops steeply at the beginning, and then decreases with increasing elapsing time and seems to approach a relaxation limit that depends on the applied strain (or stress level). Hence, in order to compare the relaxation behaviour of each series of blends and at different constant strain levels, reduced stress ($\sigma(t)/\sigma_0$) was plotted against time. At short durations, the curves decayed fairly quickly, after which the stress decay reduced markedly. The times required to reach 80% and 70% of the initial stress for each blend composition and initial stress level are summarized in Table III. These stress ratios were arbitrarily selected to enable qualitative comparison of stress relaxation behaviour of various blend compositions. From Table III it appeared that starch blends containing EVA relaxed the fastest in terms of reaching a reduced stress level of 0.8. Blends containing LDPE took the longest time to relax to the reduced stress level of 0.8. The longer relaxation of LDPE or HDPE blends is probably due to the crystallinity of these synthetic polymers. In several instances for LDPE blends, the reduced stress level of 0.7 was not reached after 2500 s. The slightly longer time required for LDPE melts to relax to a particular reduced stress level could be due to the lower mould temperature (40 °C for LDPE blends as opposed to 45 °C for HDPE blends). At higher mould temperature, there are greater opportunities for the stresses to relax. As the initial stress level, σ_0, at which the relaxation began increased, the time at which the reduced stress level of 0.8 was attained increased, and then decreased with further increase in σ_0. Imposition in the beginning of a high strain destroys the

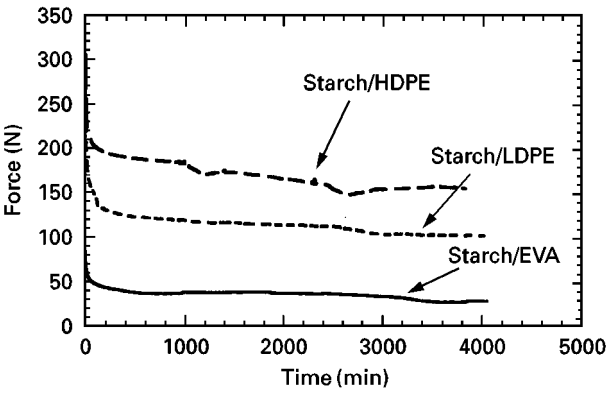

Figure 3 Force–time plot for a long-term experiment for blends containing three different types of polymer. The starch content was 60% by weight.

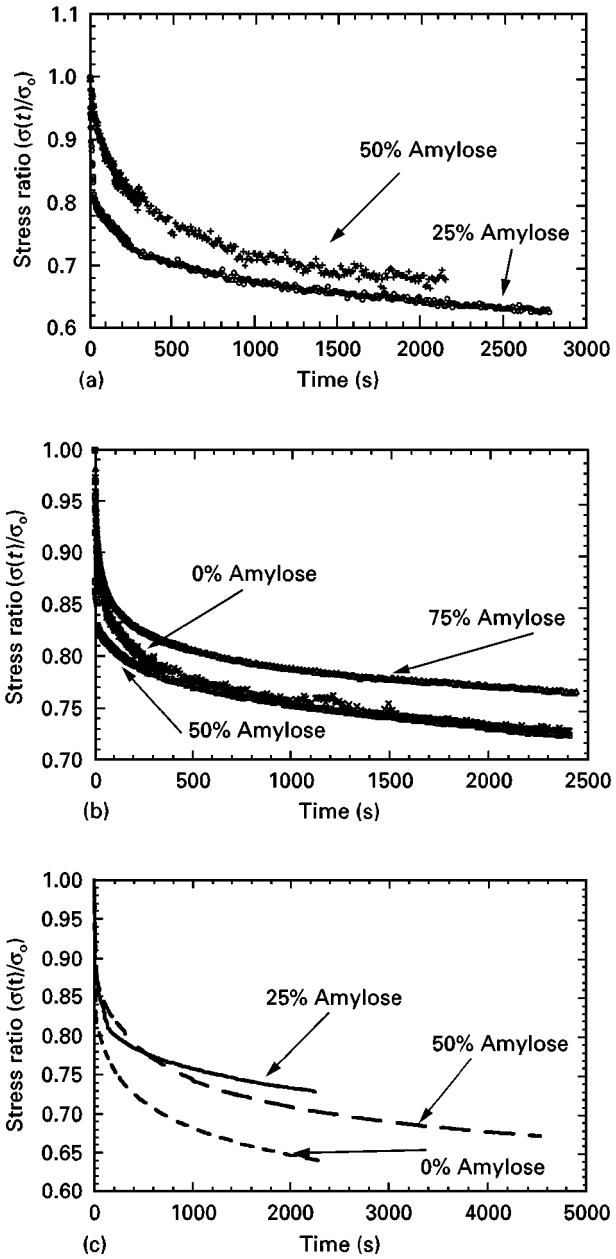

Figure 4 Stress relaxation plots ($\sigma(t)/\sigma_0$) for (a) starch/EVA, (b) starch/LDPE, and (c) starch/HDPE blends containing 70% starch of various amylose contents.

resistance of the material to deformation, resulting in a lower value of equilibrium stress. In general, as the amylose content in the blend increased, the time taken for the material to relax increased. This is possibly due to the fact that amylose, which is the linear fraction in starch, leads to greater interaction with the anhydride group in the synthetic polymer.

When the relaxation of stress, σ, as a function of logarithmic time is plotted, these materials show a sigmoidal stress relaxation similar to that of synthetic polymers. The curves consists of two regions: an initial nearly horizontal portion starting at the initial stress level, σ_0, and a linearly descending region with a constant slope. The duration of the initial horizontal portion is much shorter for the starch/HDPE and starch/LDPE blends (<10 s) than for starch/EVA. Hence, plots of log stress and log time are approximately linear over the entire range for which these tests were recorded.

The slopes of the various curves are summarized in Table IV. Starch/EVA blends have the highest slope, while blends containing LDPE have the lowest. There appeared to be no discerning effect on the level of stress or the amylose/amylopectin ratio in starch on the slope of log stress–log time plot. The parallel nature of these plots when the initial strain is varied indicates the separability of strain and time effects in viscoelastic deformation. The order of magnitude of the slope is in agreement with the published work of Bagley and Dixon [9] on starch xanthide-reinforced vulcanizates.

At longer times, the relaxation curves are best described by a power-law relation

$$\dot{\varepsilon} = \frac{\dot{\sigma}}{E} + A(\sigma - \sigma_i)^n \tag{2}$$

where σ denotes the stress, ε the strain, E is the tensile modulus, and A and n are material parameters. For stress relaxation, the above equation reduces to

$$\dot{\sigma} = \frac{d\sigma}{dt} = -EA(\sigma - \sigma_i)^n \tag{3}$$

The value of n is approximately equal to the inverse of the slope of the log stress and log time curves (Table IV) and is in agreement with those reported in the literature [9].

The effect of starch level on the relaxation behaviour of blends containing HDPE and LDPE with their respective compatibilizer is given in Table V. Fig. 5a and b show the relaxation behaviour as a function of starch content for starch/HDPE and starch/LDPE blends, respectively. It can be observed that as the starch level is increased, the time to relax to a particular stress level increased. However, no differences are observed between the stress relaxation behaviour of pure synthetic polymer and a blend containing 15% starch. Slopes of log stress–log time plots for various starch levels indicate that as the starch content is increased the magnitude of the slope decreases. For starch/EVA blends containing lower levels of starch ($<50\%$), the curves are approximately linear at the higher values of $\sigma(t)/\sigma_0$ (shorter times). For lower starch levels, the synthetic polymer is the continuous phase with starch to synthetic polymer is almost one, because the density of starch is much greater than the density of the synthetic polymer. At a higher starch levels of 70 wt %, starch occupies a volume of 63% and exists with the synthetic polymer in a co-continuous phase. Because of the higher rigidity of the starch molecules, the relaxation process is significantly hindered. Even at a modest starch level of 30 wt %, there is a slight increase in the time required to reach a reduced stress level of 0.8.

In most cases it is observed that the initial stress, σ_0, does not have a significant effect on the position of the relaxation curves ($\sigma(t)/\sigma_0$ versus t). Fig. 6 shows examples of stress-relaxation curves ($\sigma(t)/\sigma_0$ versus t) at different initial deformations. Generally, an increase in the initial elongation shifts the curves towards longer times for LDPE, while for HDPE the reverse is true.

TABLE III Characteristics of stress-relaxation behaviour for blends

Starch	Stress levels (%)	HDPE		EVA		LDPE	
		t_{80}(s)	t_{70}(s)	t_{80}(s)	t_{70}(s)	t_{80}(s)	t_{70}(s)
Waxy	20	100	[a]	[b]	[a]	40	[a]
	35	125	553	32	125	590	[a]
	50	200	2400	110	495	1150	[a]
	65	80	1500	385	[a]	238	[a]
	80	63	690	[b]	[a]	245	[a]
Normal	20	45	650	[b]	[a]	114	[a]
	35	110	[a]	150	375	45	470
	50	520	[a]	30	125	660	[a]
	65	220	[a]	95	410	105	1450
	80	225	1566	40	575	230	[a]
50% Amylose	20	54	[a]	21	180	[a]	[a]
	35	145	[a]	45	295	360	[a]
	50	300	[a]	75	511	720	[a]
	65	670	[a]	50	1550	[a]	[a]
	80	390	[a]	17	190	145	[a]
70% Amylose	20	35	975	33	90	115	1286
	35	180	[a]	33	132	[a]	[a]
	50	240	[a]	104	375	560	[a]
	65	370	[a]	295	1380	640	[a]
	80	320	[a]	[b]	[a]	630	[a]

[a] Did not reach a reduced stress level of 0.7.
[b] Did not reach a reduced stress level of 0.8.

TABLE IV Slope of log (stress–time) curves for various blends

Starch	Synthetic polymer	Average slope
Waxy (0% amylose)	Low density	− 0.034
Normal (25% amylose)	Low density	− 0.04
Med. amylose (50%)	Low density	− 0.036
High amylose (75%)	Low density	− 0.039
Waxy (0% amylose)	High density	− 0.052
Normal (25% amylose)	High density	− 0.044
Med. amylose (50%)	High density	− 0.045
High amylose (75%)	High density	− 0.042
Waxy (0% amylose)	EVAMA	− 0.078
Normal (25% amylose)	EVAMA	− 0.055
Med. amylose (50%)	EVAMA	− 0.07
High amylose (75%)	EVAMA	− 0.10

TABLE V Slope of log (stress–time) curves for HDPE and LDPE containing various starch contents

Starch contents (%)	HDPE	LDPE
0	− 0.12	− 0.078
15	− 0.104	− 0.077
30	− 0.104	− 0.076
50	− 0.086	− 0.071
60	− 0.081	− 0.064

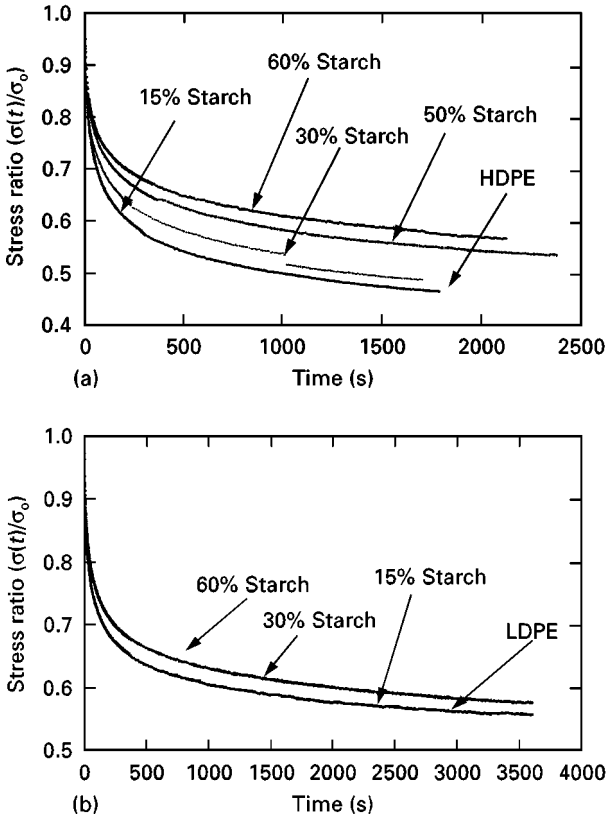

Figure 5 Stress relaxation plots ($\sigma(t)/\sigma_0$) for (a) starch/HDPE, and (b) starch/LDPE blends containing various starch contents.

This is in agreement with previously published data presented in the literature [4]. For blends containing starch/LDPE, the trend is similar to that for LDPE with a slight compression in the range of the relaxation curves. For blends containing starch/HDPE, as the initial elongation is increased, the relaxation curves have a crossover point or tend to converge at long times.

The modulus values of the rubbery starch/EVA blends can be used to calculate the two constants in the

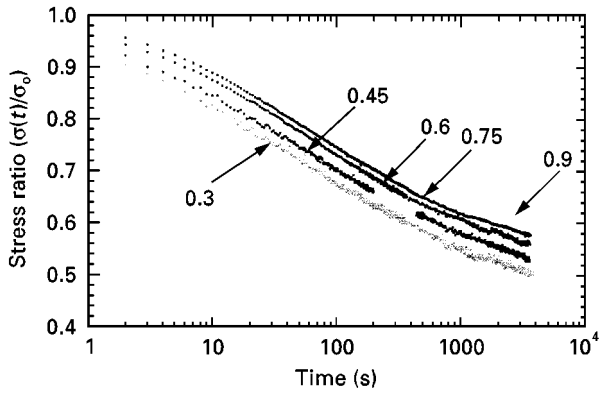

Figure 6 Stress relaxation plots ($\sigma(t)/\sigma_0$) for LDPE at various strain levels.

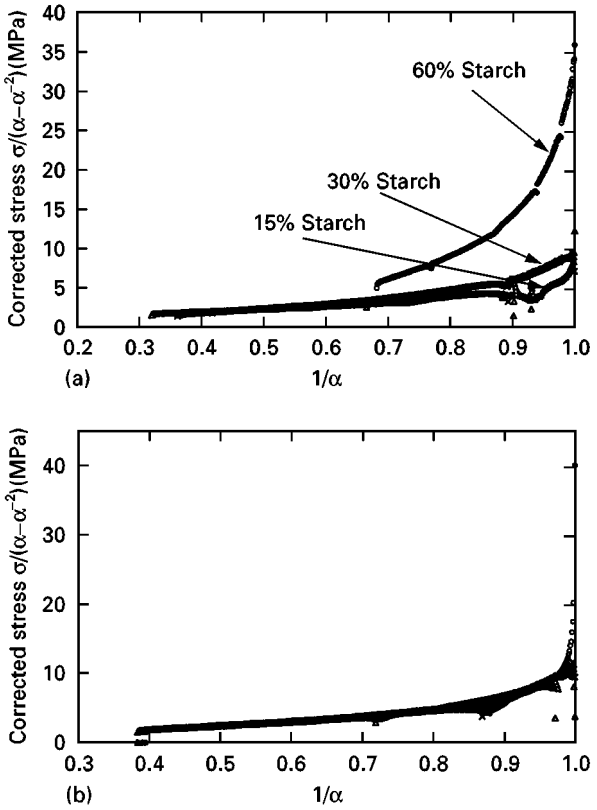

Figure 7 Mooney-plots of starch/EVA blends (a) at different starch content, and (b) at the same starch content for four different samples: (○) 1, (△) 2, (×) 3.

Mooney–Rivlin equation, given by

$$\sigma = \left(2C_1 + \frac{2C_2}{\alpha}\right)\left(\alpha - \frac{1}{\alpha^2}\right) \quad (4)$$

where the constant $2C_2$ is a measure of the departure of the observed stress–strain relationship from that predicted from molecular or statistical theory of rubber elasticity. The modulus tends towards a high value at low strains. The curves becomes extremely steep as α^{-1} approaches 1 (Fig. 7a) and hence it is difficult to estimate the constants. This is also similar to that reported by Bagley and Dixon [9] for starch xanthide-reinforced rubber. According to Hassan and Ray [10], this rapid rise in the stress values α^{-1} approaches 1 is due to the errors in evaluating the term $\alpha - (1/\alpha^2)$. Similar comments were made by Hasa and Van der Hoff [11] who emphasized the neccesity to measure the initial length of the sample very precisely. For the three replicates, the curves shown in Fig. 7b of the apparent moduli and α^{-1} are identical up to a value of $\alpha^{-1} = 0.95$, after which they deviate. Also, extrapolation of the corrected stress versus α^{-1} plot is questionable for blends containing a high percentage of starch, because data for high elongation values, α, are unavailable.

3.2. Residual stress

There are several techniques for measuring residual stresses in polymers. These include optical methods such as birefringence, which is applicable to materials that are transparent [12, 13]; or the layer-removal technique [14], which is mostly applied on rigid materials and is inapplicable to soft or semi-rigid materials as used in this study. The stress relaxation techniques offers a reasonable way of obtaining residual stresses in these materials. The relaxation behaviour of metals and polymers are fundamentally similar in that the maximum slope of the stress-relaxation curve of a solid is related to the initial stress, σ_0, and the internal or equilibrium stress, σ_i, attained after sufficiently long times. While with the birefringence and the layer removal technique it is possible to obtain the stress distribution in the sample, i.e. stress as a function of position, the stress-relaxation method is expected to produce an average value over the whole cross-section of the sample. For blends, average values would be more meaningful, as the morphology is not expected to be uniform across the cross-section, and interpretation of stress as a function of position would be difficult.

The value of σ_i obtained using Li's technique is given in Table VI. For most samples, the internal stress is negative, i.e. frozen-in compressive stress. When a polymer melt enters a mould whose temperature is significantly lower than that of the melt, the material in contact with the cavity wall and that adjacent to the wall, cool rapidly and set. The material in the interior of the mould cools much more slowly because of the lower thermal conductivity of the polymer. Owing to thermal shrinkage, a hydrostaic tensile stress is generated in the interior which must be balanced by a compressive stress in the skin. The internal stress parameter derived from Li's analysis is deformation-dependent, i.e. the total internal stress is the total sum of frozen-in internal stress developed during the moulding and the strain-dependent internal stress and stress level is not linear in this study, thus making it difficult to estimate σ_i corresponding to $\sigma_0 = 0$. In general, an increase in σ_i with strain has been reported by Kubat and co-workers for HDPE, LDPE, and molybdenum [7].

The value of σ_i obtained using the method of Kubat and Rigdahl [2–4, 15] is also given in Table VI. The magnitude of σ_i is the measure of the frozen-in internal stress. A plot of the maximum slope of stress–log(time) curves with initial stress, σ_0, is shown

TABLE VI Comparison of residual stress as obtained from Li versus Kubat–Rigdahl plot

	Residual stress (MPa)					
	Li analysis			Kubat–Rigdahl analysis		
Starch type	HDPE	LDPE	EVA	HDPE	LDPE	EVA
Waxy	− 0.60	− 0.31	− 0.07	1.84	0.558	− 0.096
Normal	− 0.07	0.27	− 0.23	0.63	− 1.91	0.267
50% amylose	− 0.24	− 0.115	− 0.122	3.76	1.346	− 0.208
70% amylose	− 0.10	0.37	− 0.30	− 0.27	− 5.67	− 5.51

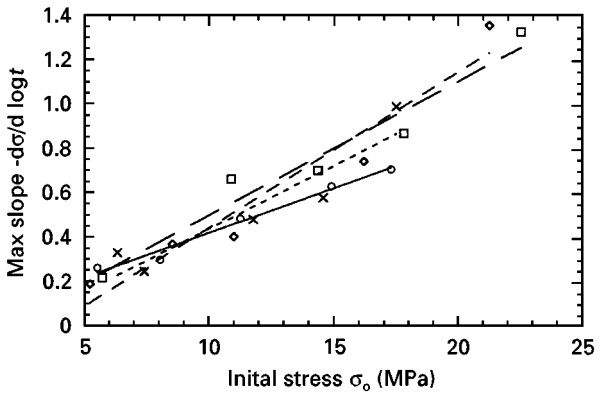

Figure 8 Kubat–Rigdahl plot for measuring residual stress for starch–HDPE blends: 70% amylose, (—□—) 0% amylose, (—◇—) 50% amylose, (- - × - -) 25% amylose.

in Fig. 8. The values of σ_i are much higher (almost by an order of magnitude in some instances) than those obtained using Li's method. The variation in σ_i values between blends of various starches is also higher compared to Li's method. This can be attributed to the scatter in the data from the KR procedure, which is much higher. The magnitude of σ_i is affected by the slope of the F_{max} versus σ_0 plot. The slope of the F_{max} versus σ_0 plot is also equal to $n^{-n/(n-1)}$ where n is the power-law index describing the stress relaxation behaviour. Large standard deviations (up to 50%) were reported by Sandilands and White [16] when determining σ_i for various injection-moulded polystyrenes. The scatter is also evident in Fig. 8 and the data presented by Haworth and White [17]. Because the per cent elongation of most of these materials is low (2%–15%), a sufficient difference in the stress levels is necessary to obtain meaningful and reproducible data. Hence, the experiment had to be conducted in the range indicated (20%–80% yield stress).

Residual stress calculated from Li-type plots as a function of starch content is summarized in Table VII. For blends containing starch and LDPE, σ_i decreases as the starch content increases. This is consistent with the findings which indicate that the blends relax to a higher equilibrium stress as the starch content increases.

The shapes of the Li-type curves are a function of the equation relating stress to time (see Equations 5–8). Fig. 9 shows the plots of Li-type curves obtained using constants associated with each of the Equations 5–8. At stress levels $(\sigma(t)/\sigma_0)$ less than 0.7, Equations

TABLE VII Residual stress obtained from Li-plots for starch/LDPE blend

Starch content (%)	Residual stress MPa
0	− 0.093
15	− 0.245
30	− 0.241
50	− 0.28
60	− 0.46

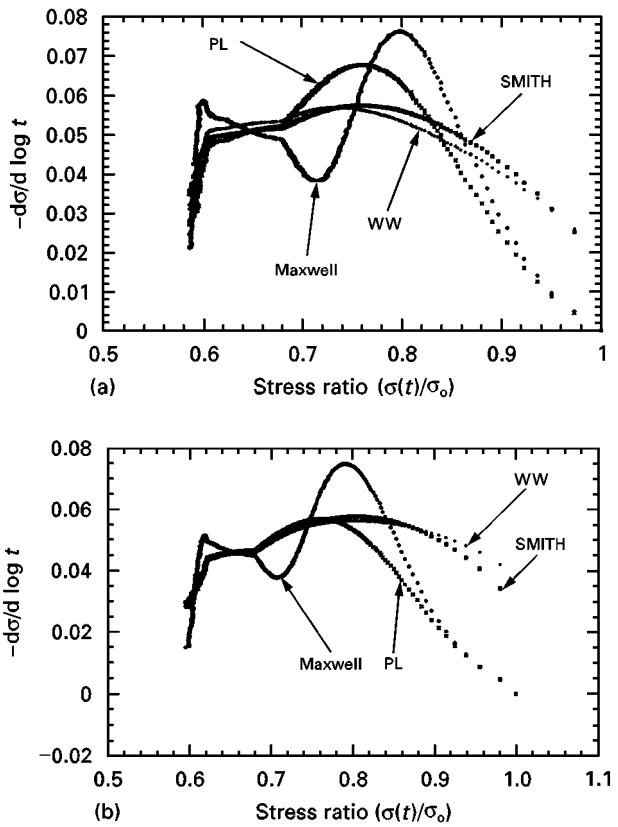

Figure 9 Comparison of Li-plots using constants from four different equations for (a) starch (50%)/LDPE (50%), and (b) starch (60%)/LDPE (40%).

6–8 produce almost identical plots. The Maxwell model produces a plot with two pronounced shoulders, each corresponding to the relaxation time constants τ_2 and τ_1, respectively, while Equations 6 and 8 produce a single broad shoulder corresponding to the relaxation time constant, τ, in Equations 6 and 8.

The maxima in the power-law plots are a function of the slope n in Equation 3.

3.3. Models

Most polymeric solids are known to show non-linear viscoelastic–plastic behaviour even in small strain ranges. Various models are available to relate the stress relaxation in polymers. Mechanical analogues are a useful way of describing viscoelastic behaviour, though the physical significance of its constants is unclear. Most of these models are non-linear and the associated constants can be fitted using a non-linear regression technique. The Maxwell model, with a series of spring and dashpots, can be represented by

$$\sigma(t) = \sigma_e + \sum_{n=1}^{\infty} \sigma_n e^{-t/\tau_n} \quad (5)$$

where σ_e is the equilibrium stress and τ is the time constant. Strictly speaking, these models are generally applicable to homopolymers. A two-Maxwell element ($n = 2$) was sufficient to fit the data. A single element was able to account for the data until $t > 1000$ s. For data between 1000 and 3000 s, a second Maxwell element is needed. As the duration of the experiment is increased, the number of Maxwell elements, required to obtain an acceptable fit, increases.

An alternate equation to represent the relaxation function is that proposed by Smith [18] where the stress is related to the time decay by the equation.

$$\sigma(t) = \sigma_e + \left\{ \sigma \Big/ \left[1 + \left(\frac{t}{\tau} \right)^k \right] \right\} \quad (6)$$

where σ is the difference between glassy or short-time stress and the equilibrium or long-time stress, σ_e, with τ and k being empirical constants. Both these models fit the data well. The time constant, τ, in Equation 5 is the highest for the EVA blends by almost an order of magnitude and lowest for the LDPE blends. The constant k ranges from 0.2–0.6. The value of σ is the highest for HDPE blends and the lowest for EVA blends. τ is generally the lowest for the lowest σ_0, except for LDPE where it decreases as σ_0 increases. As is expected, both σ_e and σ increases as σ_0 and the starch content in the blend increased.

Two other models can also be evaluated. The first is the power-law model obtained by solving Equation 3 which leads to [19]

$$\sigma(t) = \sigma_e + [(n-1)\, EAt + (\sigma_0 - \sigma_e)^{1-n}]^{1/(1-n)} \quad (7)$$

and the second is the Williams–Watts function represented by

$$\sigma(t) = \sigma_e + \sigma_0 e^{-(t/\tau)^m} \quad (8)$$

Again, both these model fit the data well. However, Equation 7 is computationally more tedious and under-predicts the stress at short times. It should also be noted that the time constant in Equations 6 and 8 are extremely sensitive to the constant k and m, while in Equation 7, B is sensitive to n. These constants control the relaxation mechanism in these blends.

Conclusion

The stress relaxation behaviour of starch/synthetic polymer blends is similar in many respects to that of synthetic polymers. Starch/EVA blends display properties similar to rubbery polymer. The modulus of the blends increased as the starch content increased. The shape of the relaxation curve (σ versus log time) is sigmoidal. "True" elastic equilibrium is seldom achieved even after a long duration. The relaxation behaviour of the blends is controlled by the relaxation mechanism of the continuous phase (in this case the synthetic polymer).

Blends containing EVA relaxed the fastest, i.e. stress approached asymptotically lower values of $\sigma(t)/\sigma_0$ at longer times, while those containing LDPE took the longest time to relax, presumably due to the combination of higher crystallinity of lower mould temperature used. As the amylose content or the starch in the blend increased, the time taken for the material to relax, increased. Logarithmic stress versus time curves for different applied strains gave plots that were parallel, indicating the separability of strain and time effects. Mooney plots for starch–EVA blends are linear for α^{-1} ranging from 0.4–0.95, after which they increase exponentially.

The Li and the KR techniques for measuring residual stress gave values that were significantly different in magnitude. The value obtained is an average over the entire cross-section. Kubat and Rigdahl [2] have suggested a three-layer model, characterizing each layer that has a different relaxation mechanism with a different power-law index n (Equation 3). A potential drawback of the KR technique is the large number of experiments that have to be conducted. The scatter in the F_{max} versus σ_0 plot makes linear extrapolation questionable, and results in the high standard deviation associated with the estimate of residual stress. The Li technique, on the other hand, is somewhat simpler and requires a single experiment but the residual stress is strain dependent. Requiring a strain-independent value of residual stress would require experimentation at several strain levels (or σ_0) and extrapolating to zero σ_0, a technique prone to the same errors as the KR plots.

Several empirical models can be used to fit the kinetics of stress relaxation well. The number of elements required in the Maxwell model increases with the duration of the experiment or until true equilibrium is reached. The Maxwell model produces a plot with two pronounced shoulders, each corresponding to the relaxation time constants τ_2 and τ_1, respectively, while the other models produce a single broad shoulder. The constants are dependent on the intial stress, σ_0, as is the stress rate, $\dot{\sigma}$.

Acknowledgement

The author would like to acknowledge the financial support of the US Department of Energy (Contract DE-FG02-96ER12185) for this work.

References

1. A. I. ISAYEV (ed.) "Injection and Compression Molding Fundamentals" (Marcel Dekker, New York, 1987) pp. 277–327.
2. J. KUBAT and M. RIGDAHL, *Int. J. Polym. Mater.* **3** (1975) 287.
3. *Idem*, *Mater. Sci. Eng.* **24** (1976) 223.
4. J. KUBAT, R. SELDEN and M. RIGDAHL, *Appl. Polym. Sci.* **22** (1978) 1715.
5. J. M. C. LI, *Can. J. Phys.* **45** (1967) 493.
6. J. KUBAT, M. RIGDAHL and M. WELANDER, *Coll. Polym. Sci.* **266** (1988) 509.
7. B. HAGSTROM, J. KUBAT and M. RIGDAHL, *J. Appl. Polym. Sci.* **36** (1988) 1375.
8. R. MANI and M. BHATTACHARYA, *Eur. Polym. J.*, in press.
9. E. B. BAGLEY and R. E. DIXON, *Trans. Soc. Rheol.* **18** (1974) 371.
10. A. M. HASSAN and L. N. RAY, *J. Appl. Polym. Sci.* **15** (1971) 1837.
11. J. HASA and B. M. E. VAN DER HOFF, *J. Polym. Sci. Polym. Phys. Ed.* **11** (1973) 297.
12. R. S. STEIN, S. ONOGI, D. A. KEEDY, *J. Poly. Sci.* **57** (1962) 801.
13. B. E. READ, *Polymer* **5** (1964) 1.
14. R. G. TREUTING, W. T. READ, *J. Appl. Phys.* **22** (1951) 130.
15. J. KUBAT and M. RIGDAHL, *Polym. Eng. Sci.* **16** (1976) 792.
16. G. J. SANDILANDS and J. R. WHITE, *Polymer* **21** (1980) 338.
17. B. HAWORTH and R. WHITE, *J. Mater. Sci.* **16** (1981) 3263.
18. T. L. SMITH, *J. Polym. Sci.* **35** (1971) 39.
19. C. G. EK, J. KUBAT and M. RIGDAHL, *Coll. Polym. Sci.* **265** (1987) 803.

Received 19 August 1997
and accepted 22 April 1998